

Organic Vapor Sensing with Enhanced Sensitivity using Polymer-coated Thickness Shear Mode Devices

Randolph D. Williams, Anant K. Upadhyayula and Venkat R. Bhethanabotla¹

Sensors Research Laboratory, Department of Chemical Engineering, University of South Florida, 4202 E. Fowler Ave., ENB 118, Tampa, FL 33620

Abstract

Thickness shear mode (TSM) sensors, also known as quartz crystal micro-balances (QCM) are a class of acoustic wave sensors that have been used for gas/vapor sensing and for determining liquid properties. Fast and sensitive chemical vapor sensing, specifically of hydrocarbon vapors, has attracted recent attention. The TSM sensors typically used have a lower sensitivity compared with other acoustic wave sensors. This paper describes the development of high sensitivity organic vapor sensors using polymer thin film coatings on TSM devices. Commercially available AT-quartz TSM devices were milled leaving a thin quartz membrane surrounded by an outer ring. This resulted in an increased frequency and a consequent increase in sensitivity, as described by the Sauerbrey equation. The TSM sensors were then coated with thin sensing films of rubbery polymers. Isothermal runs above room temperature were conducted. A fully instrumented and automated test bed consisting of a temperature-controlled organic vapor dilution system, a precision impedance analyzer, and computer based data acquisition was developed and used to evaluate the performance of the coated TSM devices. We present initial results of tests conducted to demonstrate increase in sensitivity.

1. Introduction

To construct gas or vapor sensors, chemically sorbent films are commonly coated onto TSM resonators¹. Chemical sensitivity and selectivity is imparted by attaching a thin film to the acoustically active region of the TSM device. Devices employed in this work were AT cut quartz crystals with circular gold electrodes on both sides. Because of the piezoelectric properties of the quartz material, application of a voltage between the two electrodes at the surface results in a shear deformation of the crystal. The quartz crystal then vibrates via the piezoelectric effect and this vibrational motion results in the generation of a transverse acoustic wave that propagates across the thickness of the quartz crystal. The resonant frequency of the TSM device decreases with the crystal thickness when a standing wave condition is met, as

$$t_q = \frac{\lambda_q}{2} \quad (1)$$

¹ Corresponding author: email venkat@eng.usf.edu

$$v = \left(\frac{\mu_q}{\rho_q} \right)^{1/2} \quad (2)$$

Here v is the velocity of sound in the quartz and t_q is the quartz thickness. Equation 2 gives the velocity, where ρ_q is the density (2.648 g cm^{-3}) and μ_q is the shear modulus of the quartz ($2.947 \times 10^{11} \text{ g cm}^{-1} \text{ s}^{-2}$). Since the quartz thickness is much larger than the electrode thickness, the electrodes are neglected when determining the resonant frequency. Equations have been developed to yield expressions for the dependence of the resonant frequency on the mass changes occurring within films coated onto the TSM sensor. The Sauerbrey equation² is one such relationship, valid for small mass loadings, such as in vapor sensing situations:

$$\Delta f = \frac{2f_r^2 \rho_s}{(\mu_q \rho_q)^{1/2}} \quad (3)$$

where Δf is the measured frequency shift, f_r is the resonant frequency, and ρ_s is the film density (which can be related to the film mass). Changes in the film mass will cause frequency shifts; these frequency shifts are dependent upon the film selectivity and the device sensitivity. In Sauerbrey's model, the sensitivity c_f is given by:

$$c_f = \frac{2f_r^2}{\rho_q v_q} \quad (4)$$

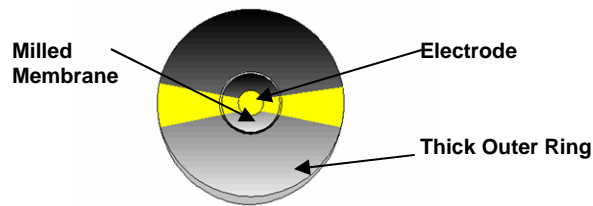
Consequently, a commonly used 10 MHz AT cut quartz crystal (with the previously mentioned physical properties) will have a mass sensitivity of $2.26 \times 10^8 \text{ Hz cm}^2/\text{g}$. The addition of material with an areal density of 4.42 ng/cm^2 will cause a 1 Hz shift on this resonator, which is easily measurable using common electronics.

Although a 10 MHz TSM sensor already has a high degree of sensitivity, it is obvious from equation 4 that this sensitivity can be considerably increased by increasing the resonant frequency. For a 56 MHz device, sensitivity increases proportional to the 2.88 power of resonant frequency have been reported for liquid sensing with the signal to noise ratio improving by a factor of 6.5³. This 2.88 power dependence is greater than predicted by Sauerbrey's model. Even with sensitivity increases predicted by the Sauerbrey model, which is more likely valid for gas phase operation, a 100 MHz device will be 100 times more sensitive than a 10 MHz one. Achieving higher frequencies requires thinner quartz crystals; this is difficult using conventional techniques. However, higher frequency devices can be produced by operating at overtones of the fundamental resonant frequency or by using milled devices⁴. Equation 5 shows that the plate thickness t_q determines the wavelength of the fundamental ($n=1$) and harmonic ($n=3, 5, 7 \dots$) resonances

$$f_n = \frac{nv}{2t_q} \quad (5)$$

where f_n is the new fundamental frequency for various thicknesses or different harmonics. Milled crystals are made thinner only in the center so that a thin quartz membrane is made with a thick outer ring allowing for mechanical stability. These higher frequency devices are long known to have improved mechanical stability and frequency to noise ratios that are better than other acoustic wave devices⁵. Chemically milled devices specifically designed for our experiments, with fundamental frequencies of approximately 98 MHz having 20 mils electrode diameter were fabricated at Piezo Technology, Inc. We are in the process of fabricating various devices in the 30 MHz to 100 MHz range using the same milling techniques for these studies. A diagram of a milled TSM device is shown in Figure 1 below.

Figure 1. Milled TSM Device



2. Experimental

2.1 Experimental Apparatus

Organic benzene, toluene and dichloromethane vapor samples were generated at specific concentrations to test the coated TSM sensor. A dynamic method of generating vapor samples was used⁶. The equipment was fully automated and a schematic is given below in Figure 2.

Figure 2. Vapor Generating Apparatus

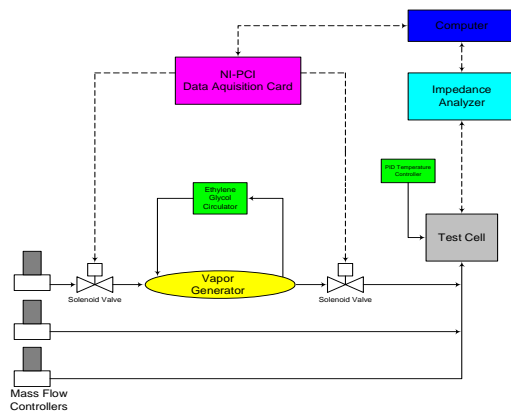
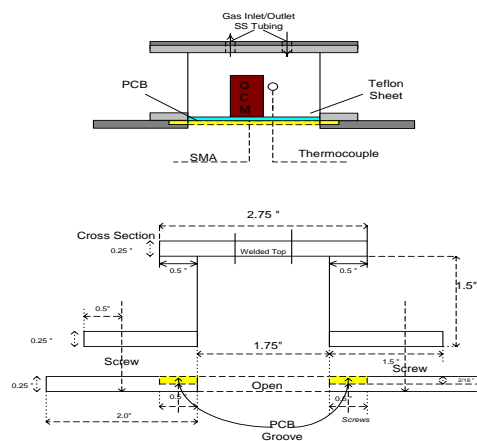


Figure 3. Test Cell



Organic liquids were contained in three of the four bubbler units housed in a temperature bath. MKS mass flow controllers were used to regulate nitrogen carrier gas through the bubbler unit. Multiple mass flow controllers allowed for a variation of test sample concentrations. In the present design, there are three streams: The carrier stream (Q_{cs}) passing through the bubbler, and the dilutant streams (Q_1 and Q_2). The vapor pressure of the liquid at the bubbler temperature is calculated using an accurate vapor pressure correlation. The mole fraction Y_s is approximated from the volume of the vapor generated (Q_s), assuming saturation of the exiting vapor from the bubblers. The generated vapor is further diluted and a new diluted mole fraction (Y_{ds}) is calculated. This mole fraction is equated to the volume fraction and then the concentration is approximated with the ideal gas law. An Agilent 4294 A Precision impedance analyzer was used to monitor the resonant frequency and equivalent circuit parameters of the TSM device. A custom made stainless steel test cell, shown in Figure 3, was designed for housing the sensor and was kept under temperature control. The TSM device was attached to a printed circuit board using a commercially available socket holder for 10 MHz resonators and a transistor socket for higher fundamental frequency resonators. The sockets facilitated easy removal of the sensor without disturbing electrical connections.

2.2 Coating

TSM devices were coated according to the spray coating method utilizing a spray brush⁷. A dilute solution of the coating (0.1 %) was aspirated through an atomizing nozzle using compressed nitrogen gas. In our first test of the apparatus, poly(vinyl) acetate was used which was obtained from Polysciences of 90,000 molecular weight. The atomized droplets impact the device surface, and the volatile solution evaporates to leave the polymer coating. Polymer coatings formed using this method may have irregular texture and coverage, however, thicknesses were reproducible because the device frequency was monitored throughout the coating process. Polymers were coated equally onto each side of the 10 MHz and 20 MHz TSM resonator for a targeted total of 3.5 kHz, to achieve quick equilibrium. The device was allowed to air dry after each coating application, and was cured to anneal the film. Resonators of 98 MHz frequency were fragile and shattered during spray coating, consequently, the polymer was coated with a more delicate technique for these resonators. A pipet was used to drop 3 to 5 microliters of the polymer solution onto each face of the resonator. The frequency and equivalent circuit parameters of the uncoated device were recorded before and after application of the polymer. Also, the resonant frequency of the device was monitored with time throughout the sorption and desorption of the vapors in the polymer.

2.3 The TSM Devices

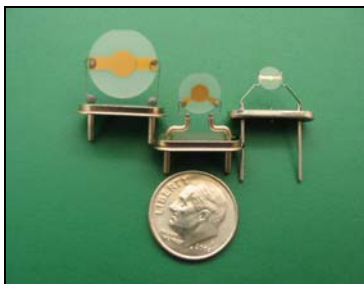
All crystals were AT cut quartz with chromium and gold electrodes. The electrode diameter of the 98 MHz device was 20 mils, the blank diameter was 200 mils and the membrane diameter was approximately 100 mils. The properties of the resonators fabricated so far, and employed in this study are given in Table 1.

Table 1. Parameters of the TSM Devices

Resonator	Blank Diameter (cm)	Electrode Diameter (cm)	Electrode Thickness (Å)	Electrode Material	Milled Area (cm ²)
10 MHz	1.367	0.5105	1000 / 100	Au / Cr	-
20 MHz	0.8077	0.3480	1000	Au/Cr	-
98 MHz	0.508	0.0508	-	Au/Cr	0.0507

These higher frequency crystals were fabricated using chemical milling. The resonator quartz blanks were etched in NaOH.0.5H₂O at 180 °C. Additionally, the 98 MHz resonators were fabricated with ring thicknesses of approximately 50 µm and membrane thicknesses of approximately 17 µm. A chemically milled 98 MHz resonator is shown in Figure 4.

Figure 4. 5 MHz (left), 20 MHz (middle), and 98 MHz TSM Devices (right)

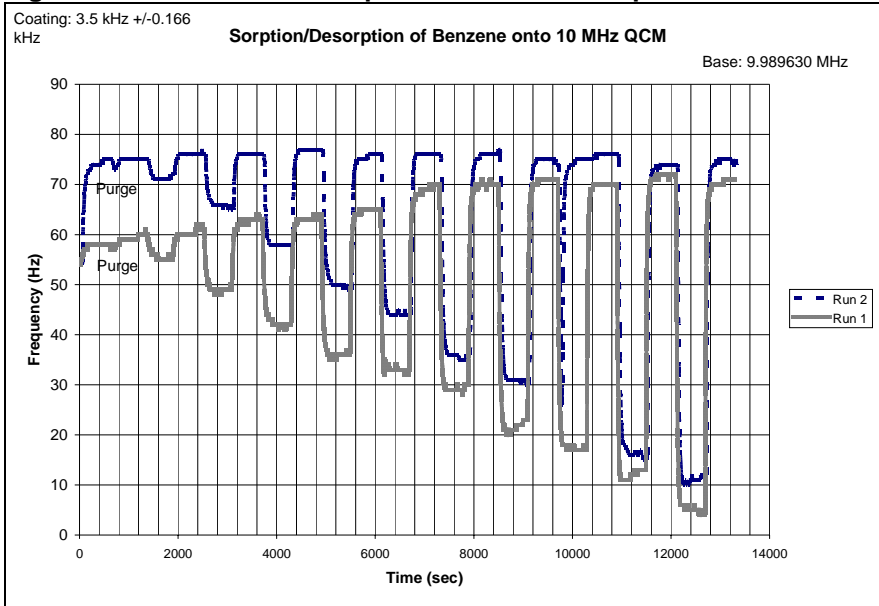


3. Preliminary Results

Each of the resonators in Table 1 were exposed to various concentrations of benzene after being coated with poly(vinyl) acetate. The frequency responses of the sensor were recorded during exposure to compare sensitivities. The concentration was increased in step values from 9894 mg/m³ to 96377 mg/m³, with purges between each concentration to allow the film to recover. Results for 10 MHz and 20 MHz devices are presented here. A total flow rate of 280 sccm was always maintained over the surface of the device. The temperature of the cell and the lines were maintained at 50 °C. Initial results revealed that the polymer coated onto the device was too thick (approximately 20 kHz), consequently, equilibrium could not be attained within a short time interval. Polymer coatings of poly(vinyl) acetate (3.5 kHz or 111 nm onto a 10 MHz device and 6.5 kHz or 61 nm onto a 20 MHz device), however, reached equilibrium within a shorter time interval. Frequency measurements taken using Labview and the Agilent impedance analyzer were accurate to within 1 Hz. Readings

were stable to within ± 3 Hz. Shifts in the resonant frequency due to sorption and desorption of benzene at several concentrations are presented in Figure 5.

Figure 5. 10 MHz Device Response to Benzene Vapors



A 280 sccm nitrogen gas stream was used to purge all the lines for approximately 1300 seconds prior to exposing the polymer coated device to benzene vapors. After each exposure, the lines were again purged for 600 seconds to remove any benzene residue in the lines and to allow desorption of benzene. The first experimental run, Run 1 in Figure 5, shows that the resonant frequency initially returned to its initial frequency after the first exposure. It was observed that switching solenoid valves caused initial spikes of 1 to 3 Hz in the frequency. The frequency shifts for a 10 MHz device, corresponding to each concentration are shown in Table 2. A second experiment was used to check the reproducibility of the sensor response, however, changes in the film due to the first experiment caused a shift in the base resonant frequency, suggesting the need for improvements in coating procedures.

Table 2. Frequency Shifts Due to Benzene Sorption onto 10 MHz QCM

Concentration (mg/m^3)	Frequency Shift (Hz) (Run 1)	Frequency Shift (Hz) (Run2)
9894.014	9	3
19729.721	10	9
29507.634	18	16
39228.260	24	23
48892.103	28	27
58499.658	35	35
68051.416	43	40
77547.861	48	3
86989.472	52	56
96376.723	60	56

Figure 6. 20 MHz QCM Response to Benzene Vapors

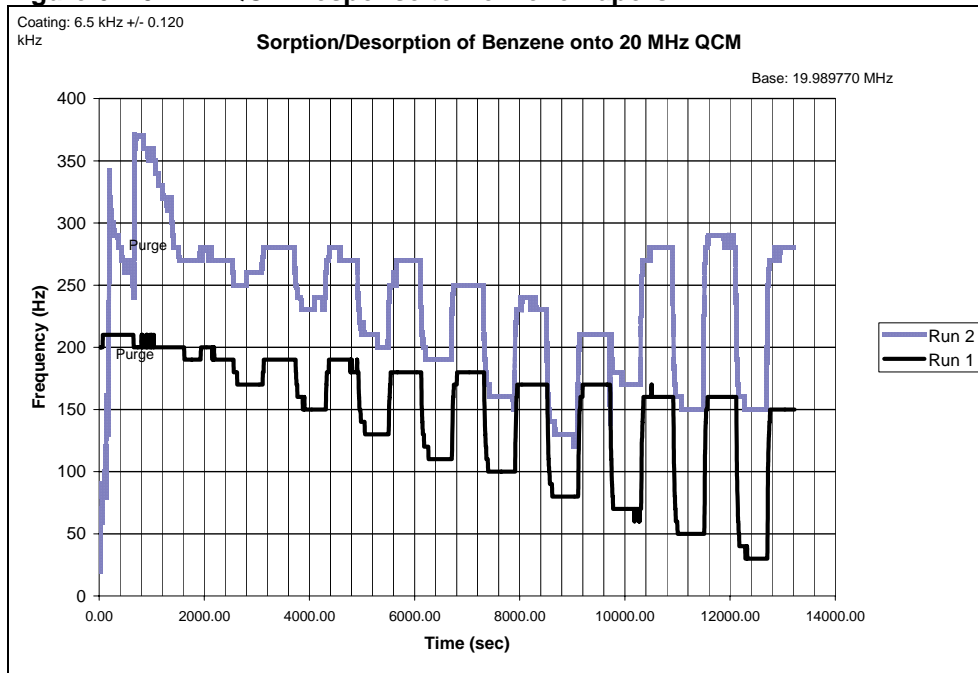


Figure 6 shows the 20 MHz device response to benzene. The same concentrations of benzene used for the 10 MHz runs were used with a similar procedure of exposure followed by purging with nitrogen. Once again, the second experiment, Run 2, has a higher base frequency than Run 1 due to effects of the first run on the same polymer film.

Conclusions and on-going work

In our efforts to demonstrate utilization of higher frequency TSM devices in vapor sensing experiments, we have constructed a test bed and a vapor generation system. 98 MHz TSM devices have been successfully fabricated using chemical milling techniques. It is found that more delicate techniques for depositing the polymer layer than spray coating are necessary for these high frequency devices. Limited tests conducted on the lower frequency devices (10 and 20 MHz) revealed that improvements to polymer adhesion are necessary. Devices in the 20 to 100 MHz range in steps of 20 MHz are currently being fabricated. Alternative techniques to coat the higher frequency devices, and to promote polymer electrode adhesion are also under development. We expect to complete this work soon to present the results.

References

1. Martin, S. J.; Frye, G. C.; Wessendorf, K. *Sensors and Actuators A* 1994, 44, 209-218.
2. Sauerbrey, G. *Zeitschrift Phys* 1959, 155, 206-222.

3. Uttenthaler, E.; Schräml, M.; Mandel, J.; Drost, S. *Biosensors and Bioelectronics* 2001 16, 735-743.
4. Neumeier, D. A. 2002 IEEE International Frequency Control Symposium and PDA Exhibition; 2002, pp 394-402.
5. Guttwein, G. K.; Ballato, A. D.; Lukaszek, T. J. VHF-UHF Piezoelectric Resonators. U. S. Patent 3,694,677; Sept 26, 1972.
6. Grate, J. W.; Ballantine, D. S.; Wohltjen, H. *Sensors and Actuators* 1987, 11, 173-188.
7. Ballantine, D. S.; White, R. M.; Martin, S. J.; Ricco, A. J.; Zellers, E. T.; Frye, G. C.; Wohltjen, H. *Acoustic Wave Sensors: Theory, Design and Physioco-Chemical Applications*; Academic Press: San Diego, 1997.